Task and motion plannig for Selective Weed Conrol using a Team of Autonomous Vehicles

I A Hameed*; A la Cour-Harbo; K D Hansen

Aalborg University, Faculty of Engineering and Science, Dept. of Electronic Systems, Section of Automation and Control, Fredrik Bajers Vej 7C, 9220 Aalborg, Denmark
* Corresponding author: ih@es.aau.dk

***Abstract*— Conventional agricultural fields are sprayed uniformly to control weeds, insects, and diseases. To reduce cultivation expenses, to produce healthier food and to create more environmentally friendly farms, chemicals should only be applied to the right place at the right time and exactly with the right amount. In this article, a task and motion planning for a team of autonomous vehicles to reduce chemicals in farming is presented. Field data are collected by small unmanned helicopters equipped with a range of sensors, including multispectral and thermal cameras. Data collected are transmitted to a ground station to be analyzed and triggers aerial and ground-based vehicles to start close inspection and/or plant/weed treatment in specified areas. A complete trajectory is generated to enable ground-based vehicle to visit infested areas and start chemical/mechanical weed treatment.**

Keywords—path planning; turning trajectory; motion control; ASETA;

I. INTRODUCTION

Adaptive Surveying and Early treatment of crops with a Team of Autonomous vehicles (ASETA) is a research projected funded by the Danish Council for Strategic Research and aims to explore the efficient and safe task execution and cooperation between a number of ground-based and airborne vehicles and its use in the early detection and treatment of weeds in row crops e.g. sugar beets [1]. In traditional automated weed control systems, unmanned ground vehicle (UGV) scans the surface of the entire field area and identify weed species and treats it chemically or mechanically directly. The main disadvantage of these approaches is that the robot has to scan or comb the whole field looking for weed spices which is a time consuming and costly process and in addition, more crop plants are most likely to be subjected to a potential full or partial damage. In this project, surveillance is carried out based on small unmanned helicopters equipped with a range of sensors, including multispectral and thermal cameras. A path-planning algorithm for efficient unmanned aerial vehicles (UAVs) guidance based on a predefined set of waypoints and dubbin curves is used [2]. The helicopters scan large field areas, data collected are transmitted to a ground station, which analyses the data and triggers aerial and ground-based vehicles to start close inspection and plant treatment in specified areas. Small-scaled helicopters are used to provide the system with multi-spectral aerial images. Using data from the helicopters, the system identifies infestations and intensive weed spots in the field and then dispatches autonomous ground vehicles to the infestations to exactly identify and localize the weeds [1-3].

UGVs require high-precision control, continuous operation, increased efficiency, and the removal of a human operator from an unsafe environment. Although autonomous vehicles have been for long the subject of research, only recently have sensor and computer technology made autonomous vehicles practical [4]. The advent of Global Positioning Systems (GPS) sensors which has offered engineers the high precision necessary for accurate vehicle control and the relatively inexpensive computers which are capable of running complex control and estimation algorithms make it practical for real-time control. With all the tools necessary for economical real-time land-vehicle control, specific commercial applications are stimulating research into effective vehicle control systems. Agriculture has emerged as one of the first potential applications of real-time vehicle control. Certain types of repetitive farming tasks such as seeding, spraying, fertilizing, weed control, and harvesting could benefit from high-precision control, control which is available in all visibility conditions [4].

In this paper, a motion planning and control approach to give the UGV the capabilities to visit weed spots in the optimized manner is developed. This includes; 1) the generation of a path which follows the crop rows to minimize crop damage, 2) the generation of an optimized turning path at the end of crop rows to join rows and to enable a UGV to drive smoothly between these rows in a manner which reduces soil compaction, operational time and total travelled distance in the field, and 3) a trajectory following controller, namely the Helmsman Controller (HC), to follow the desired trajectory is proposed.

The entire work is organized as follows; we first introduce the mechanical specification of the UGV platform used in ASETA project (see Fig. 2) in Section 2.2. The dynamic model of the used UGV is presented in Section 2.3. In section 2.4, two controllers are presented. A Field coverage approach is introduced in Section 3.1. In Section 3.2, an approach for assigning rows which are the closest to the weed spots are presented. Different types of turning trajectory generation for a blind turning are presented in Section 3.3. Finally, the developed approach is tested and validated through a number of simulation experiments are performed to evaluate the tracking performance of the robot under different field and operational conditions. Finally, a brief concluding remarks and future work in Section 5 are presented.

II. UNMANNED GROUND VEHICLE (UGV) PLATFORM

A. RobuRoc Robot

The provided Unmanned Ground Vehicle (UGV) is a commercial four wheel skid steering vehicle called RobuROC-4 from Robosoft®, four-wheel drive (4WD) vehicle with custom on board computer, sensor suite, and camera setup as it is shown in Fig. 1. This robot is built for outdoor use and has 4 independent wheels mounted. They are powered by 4 brushless DC motors working together two on the left and two on the right, making the robot able to turn on the spot. The top speed is rated to 2 m/s and its weight is approximately 140 kg and up to 100 kg extra payload can be added [1]. The robot has an embedded controller, called RobuBOX, running Windows XPe. The robot is equipped with odometer, proxymeter, and a bumper sensor. The robot has a wireless emergency stop and can be driven in two modes, by a Xbox360 wireless gamepad or robuBOX commands. The commands can be sent by a UDP connection to the robot via Ethernet, and can be used for setting angular and linear velocities, and requesting data from sensors in the RobuROC-4. The sensor data is returned from the robot at a specified rate (e.g., 10 Hz).

Fig. 1. UGV platform.

B. Robot Controller

The main goal of this section is to develop a controller to enable the robot to follow a predefined trajectory under normal field conditions. Two controllers are developed and used simultaneously; one for speed control (i.e., open-loop trajectory following controller) and the second one is for position control (i.e., Helmsman controller). Block diagram of the robotics feedback control system is shown in Fig. 2.

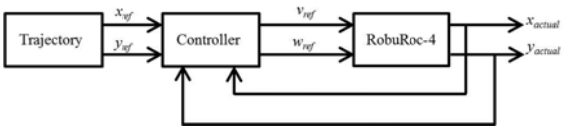

Fig. 2. Robot control system where v_{ref} and w_{ref} are the desired linear and angular velocities.

A trajectory following controller (TFC) is developed in two ways; (1) Open loop control form where the desired heading angle and consequently the desired angular and linear velocities are obtained from the reference trajectory through differentiation, and (2) Closed loop control form based on Helmsman controller principal, shown in Fig. 3. In the lower level, two PI controllers are used to regulate the linear and angular speeds of the vehicle motors.

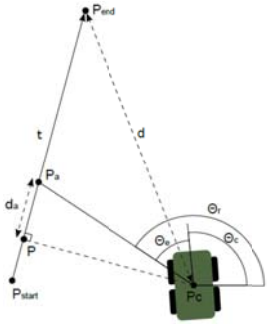

Fig. 3. Helmsman controller principal [1].

In Helmsman controller, two standard PI controllers are used for adjusting the vehicle's linear and angular speed in a manner which reduces the distance error, d (m), and heading angle error, θ_e, respectively, where P_{start} is the start waypoint of the current segment, P_{end} is the target waypoint, P_a is the aiming point on the current line segment t, P_c is the vehicle's current position, and P is the projection point of P_c on line segment t. d is the distance from the vehicle's current position to the target position (m), d_a is the distance from aiming point to the projection point (m), θ_r is the reference angle, θ_c is the current heading angle of the vehicle.

III. TASK AND MOTION PLANNING APPROACH

A. Mission planner

The system consists of a UGV and an unmanned airborne vehicle (UAV). Each vehicle has allocated a great deal of onboard autonomy and provided with a high level controller that is capable of performing its own behaviors path planning, mission execution, and obstacle avoidance. However, the coordination between these vehicles was handled by a centralized component known as the mission planner. The primary purpose of the mission planner is to provide the system with a mechanism of which allows it to carry out tasks with a high degree of autonomy. The process starts by selecting a field, scanning it using UAV, collecting data and sending it to a Ground Station (GS) where data analysis takes place, sending coordinates of weed spots back to the UAV and UGV for further inspection and then task execution, as it is shown in Fig. 4.

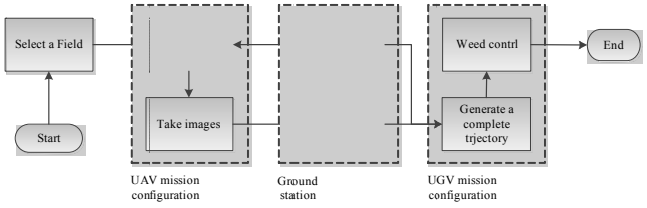

Fig. 4. System block diagram.

B. Path planning

Field coverage is the process in which field tracks and headland paths are generated in a manner to cover the whole field area. In recent years, many field coverage approaches have been developed to generate an optimized coverage path regardless of the complexity of the field shape and the presence of obstacles [4-7]. Different techniques have been developed to optimize field operations in a manner which minimizes operational time, cost and maundering over field area [8-10] through optimizing is first generated in terms of the driving angle and operating width of the vehicle. First the field is geometrically represented; a tool developed by Hameed et al. is used [7]. The 2D geometrical representation of a field involves the generation of a geometrical map which is made up by discrete geometric primitives, such as points, lines, and polygons, providing a concise representation of the environmental data that can be readily used for operational planning. The input consists of the set of coordinates of the points on the field boundary, the operating width of the implement, the number of headland paths, and the tested driving direction. The tool generates the set of the parallel field-work tracks (i.e., rows) for the complete field area coverage and gives as an output the coordinates of the points representing the starting and the ending point of each track or row, and of the points representing the headland paths, as it is shown in Fig. 5.

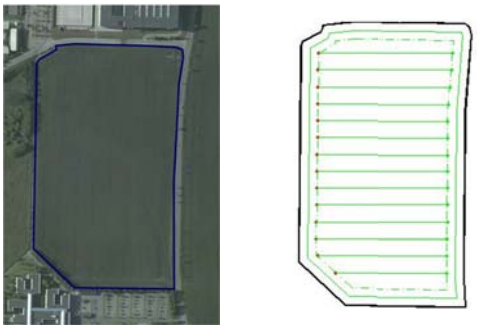

(a) (b)

Fig. 5. Example implementation of the 2D geometrical field representation: (a) Satellite image of a field of an area of around 4.5 ha located at (57° 0' 51.56" N, 9° 59' 32.97" E) with the outer field boundary in blue (b) The geometrical representation of the field for an operating width of 20m, a driving angle of 0, and a single headland path

C. Trajectory Generation

In this section, a complete trajectory to enable the vehicle to visit the intensive weed spots is generated. First the closest field rows or tracks from the weed spots are selected and ordered in a manner which reduces the total driving distance and the maneuvering over headland area. Second, turnings between the selected and ordered field rows are generated and combined with the rows to create a complete trajectory to guide the UGV through the execution of the weed control operation. Complete trajectory generation is carried out through the following steps:

1) Rows assignment

A set of coordinates representing the locations of the intensive weed spots is obtained from the helicopter. Each weed spot is assigned to a track where the vehicle can use to reach that spot. The perpendicular distances between crop row, i, and weed spot, j, are calculated using the formula given by Eq. (1). The spot with less perpendicular distance, d_{ij}, to that crop row is assigned to that particular row.

$$d_{ij} = \left\| \left(t_{x_i}, t_{y_i} \right) - \left(w_{x_j}, w_{y_j} \right) \right\|_2 \quad (1)$$

2) Connecting selected crop rows

At the end of each track the vehicle has to turn to enter to the next track. Relying on vision system to carry out a successful and safe turning is not reliable under some weather conditions. Also, sharp turnings should be avoided even if the robot is of the omnidirectional type which can turn around its center point because this type of turning can cause severe damage to soil structure and plants. In addition, a sharp turning may not be possible due to the mechanical restrictions of the vehicle and therefore a soft turning type which reduces maneuvering over headland area is required. In this paper, some typical turning types, shown in Fig. 6, will be used to join selected crop rows in a manner which reduces total travel distance and operational time [11].

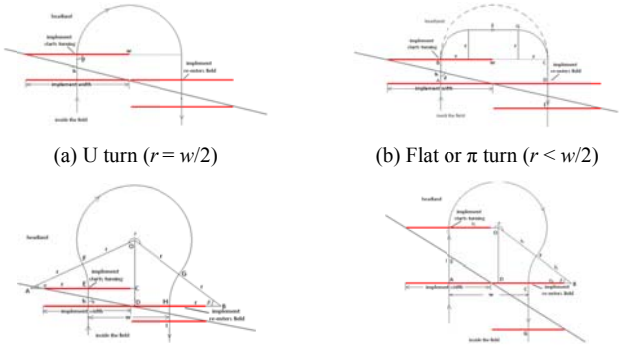

(a) U turn ($r = w/2$) (b) Flat or π turn ($r < w/2$)

(c) Bulb or Ω turn ($r > w/2$) (d) Hook turn ($r > w/2$)

Fig. 6. Turning types where r is the minimum turning width of the vehicle and w is the distance between crop rows [11].

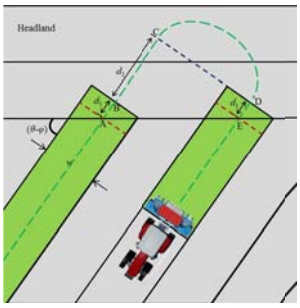

Fig. 7. Alignment of crop rows before the vehicle starts to turn; w is the implement width, θ is the driving or tracks angle and φ is the headland or edge direction [9].

3) Rows alignment

Before a turning trajectory is generated, rows must be aligned in order to carry out a successful turning. When the

centre point of the implement, shown in Fig. 7, reaches point A, a part of the implement started to exit the interior of the field. However, in order to completely finish the coverage of the current swath or track, the vehicle needed to keep moving straight ahead until point B was reached. The vehicle cannot make a turn until both tracks are aligned by keep moving until point C is reached. The vehicle then made a turn from C to D, and starts to re-enter the field from D, until the entire width of the implement was inside the field at point E. Distances d_1 and d_2 are computed using the formulas given by Eq. (2).

$$d_1 = w/\left(2\times\tan\left(\theta-\varphi\right)\right)$$
$$d_1 + d_2 = norm(\mathrm{C}-\mathrm{D})/\tan\left(\theta-\varphi\right) \quad (2)$$

IV. RESULTS

The field shown in Fig. 5 is used to demonstrate the functionality of the developed approach. A simulated set of UTM coordinates representing the locations of the weed spots which are supposed to be received from a helicopter is shown in Fig. 8(a). For a minimum turning radius, r = 10m, a trajectory with simple turning types is generated as it is shown in Fig. 8(b) where only U and flat turning types are employed. For r = 15m a trajectory with more complex turning types using U and Ω turning types is generated as it is shown in Fig. 8(c). One drawback of the current approach is that the turns may be carried out outside the headland area, as it is shown in Fig. 8(c). Enlarging the headland area or increasing the number of headland paths could be used to maneuver the UGV without going outside the headland.

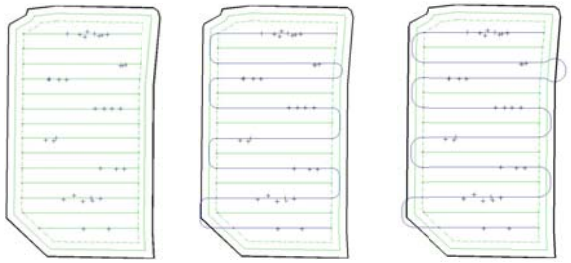

(a) (b) (c)

Fig. 8. (a) Coordinates of intensive weed spots received from a helicopter scanning the field, (b) a complete trajectory with U and flat turnings for r = 10 m, and (c) a complete trajectory with U and Ω turnings for r = 15 m.

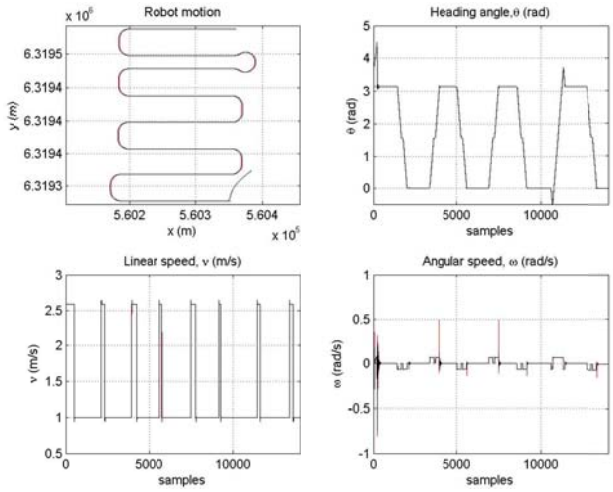

Fig. 9. Robot motion in case of using other turning types such as U, π and Ω turning curves (the robot initial position is at +57° 0' 48.42", +9° 59' 39.72" with a heading angle of 108°) where reference values are in red and actual values are in black.

The trajectory following controller is tested for a trajectory obtained for r = 15m where the controlled helped the robot model to follow complex turning shapes of U and Ω turning types as it is shown in Fig. 9. The actual and reference positions of the robot, heading angles, linear and angular speeds are shown in Fig. 9. The robot has also been tested in the real field trial starting from two different initial positions as it is shown in Fig. 10 a & b. The minimum turning distance of the robot was chosen to be 5 m and therefore a bulb- or Ω-turning type was obtained. The Helmsman controller was able to guide the robot from its initial position to the desired track and move in straight line to the other end of the track (i.e., crop row). At the end of the current track, a buld- or Ω-turning was generated and used to guide the robot through a smooth turning over the headland area. At the end of the turning trajectory, the robot entered the next track (i.e., next crop row) and the controller showed a good ability to drive the robot it in a straight line to the other end of the track.

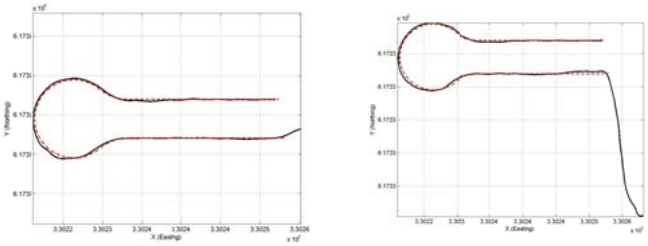

(a) (b)

Fig. 10. Testing the robot's ability to follow a trajectory from two different initial positions: desired trajectory is in dotted red line and actual robot trajectory is in solid black line.

V. CONCLUSIONS

In this paper, a novel approach for generating a complete operational trajectory to enable unmanned ground vehicle to visit specific infested weed spots identified from aerial images for a crop field is presented. A complete trajectory consists of

the selected crop rows and the turning path connecting these rows is generated to enable an unmanned ground vehicle to visit these weed spots in an optimized manner. Four types of turning types; namely, U-, π-, Ω-, and hook- turning types are generated and used to join selected crop rows. To enable a robot to follow a predefined trajectory, a trajectory following controller based on Helmsman controller principal is proposed. Simulation results showed that the controller is capable of accurately steering the robot to follow complex trajectories and reducing the tracking error under different operational conditions. An experimental field test showed that the developed controller is capable of following a predefined trajectory with high accuracy. In future work, the trajectory will be extended to 3D dimensional space in order to improve the controller performance for different field terrains.

REFERENCES

[1] A. la Cour-Harbo, "ASETA Project – Adaptive Surveying and Early treatment of crops with a Team of Autonomous vehicles," retrived from URL http://www.aseta.dk, 2010.

[2] K.D. Hansen, F. Garcia-Ruiz, W. Kazmi, M. Bisgaard, A. la Cour-Harbo, J. Rasmussen, and H.J. Andersen, "An Autonomous Robotic System for Mapping Weeds in Fields", 8th IFAC Symposium on Intelligent Autonomous Vehicles, Austrial, 2013, 217-224.

[3] W. Kazmi, M. Bisgaard, K.D. Hansen, F. Garcia-Ruiz, and A. la Cour-Harbo, "Adaptive Surveying and Early Treatment of Crops with a Team of Autonomous Vehicles," In: *Proceedings of the 5th European Conference on Mobile Robotics*, 2011, 253–258.

[4] T. Bell, "Precision robotic control of agricultural vehicles on realistic farm trajectories," Doctoral dissertation, Stanford University, Stanford, CA, 1999.

[5] T. Oksanen, and A. Visala, "Coverage path planning algorithms for agricultural field machines", *Journal of Field Robotics*, 2009, 26(8), 651-668.

[6] S. Choudhury, and S. Singh, *"A Coverage Planning Algorithm for Agricultural Robots*", Technical Report, IIT Kharagpur, India, 2009.

[7] I.A. Hameed, D.D. Bochtis, C.G. Sørensen, and M. Nøremark, "Automated generation of guidance lines for operational field planning," *Biosystems Engineering*, 2010, 107(4), 294–306.

[8] I.A. Hameed, D.D. Bochtis, and C.G. Sørensen, "Driving angle and track sequence optimization for operational path planning using genetic algorithms," *Applied Engineering in Agriculture*, 2011, 27(6), 1077-1086.

[9] J. Jin, and L. Tang, "Optimal coverage path planning for arable farming on 2D surfaces", *Transactions of the ASABE*, 2010, 53(1), 283-295.

[10] A.A. Bakhtiari, H. Navid, J. Mehri, and D.D. Bochti, "Optimal route planning of agricultural field operations using ant colony optimization", *Agricultural Engineering International: CIGR Journal*, 2011, 13(4), 1-16.

[11] J. Jin, "*Optimal field coverage path planning on 2D and 3D surfaces*," Graduate Theses and Dissertations, Iowa State University, 2009, paper 11054.